metals

MDPI

Article

The Influence of Reagents on the Shape, Stability, and Toxicity of AgNPs and Their Use to Produce Polymer-AgNPs Composites

Oksana Velgosova [1,*], Lívia Mačák [1], Vladimír Mára [2], Erika Múdra [3], Marek Vojtko [3], Maksym Lisnichuk [4] and Elena Čižmárová [2]

1 Institute of Materials and Quality Engineering, Faculty of Materials Metallurgy and Recycling, Technical University of Košice, Letná 9/A, 042 00 Košice, Slovakia; livia.macak@tuke.sk
2 Department of Materials Engineering, Faculty of Mechanical Engineering, Czech Technical University in Prague, Karlovo nám. 13, 121 32 Prague 2, Czech Republic; vladimir.mara@fs.cvut.cz (V.M.); elena.cizmarova@fs.cvut.cz (E.Č.)
3 Slovak Academy of Sciences, Division of Ceramic and Non-Metallic Systems, Institute of Materials Research, Watsonova 47, 040 01 Košice, Slovakia; emudra@saske.sk (E.M.); mvojtko@saske.sk (M.V.)
4 Faculty of Science, Institute of Physics, Pavol Jozef Šafárik University in Košice, Park Angelinum 9, 040 01 Košice, Slovakia; maksym.lisnichuk@upjs.sk
* Correspondence: oksana.velgosova@tuke.sk; Tel.: +421-55-602-2533; Fax: +421-55-602-2770

Abstract: The aim of this work was to propose a simple method for synthesizing differently shaped AgNPs and to find a suitable stabilizing/capping agent to ensure the non-toxicity of AgNPs. Using a chemical method, by simply changing the volume of reducing agents, we successfully prepared colloids of differently shaped AgNPs (spherical (~10 nm), triangular (~40 nm), rodlike (~30 nm), and a mixture of these shapes). The nanoparticle sizes and shapes affect the solution color. UV-VIS spectroscopy was used to evaluate the colloidal solutions, and transmission electron microscopy was used to analyze the shape and size of the nanoparticles. To create non-toxic and stable AgNPs, it is necessary to modify the surface properties of the nanoparticles; one possibility is to create a biocompatible layer on the nanoparticle surface. We successfully applied a combination of trisodium citrate and polyvinylpyrrolidone, thereby preventing the release of silver ions, which are responsible for the toxic effects of AgNPs. The synthesized nanoparticles show very low, mostly negligible antibiofilm activity against the green algae *Chlorella kessleri*. AgNPs were used to prepare polymer-AgNP composite thin layers and fibers. It was proved that AgNPs can influence polymer matrix properties.

Keywords: chemical synthesis; silver nanoparticles; UV-VIS spectroscopy; TEM; long-term stability; toxicity; polymer-AgNP composite

check for updates

Citation: Velgosova, O.; Mačák, L.; Mára, V.; Múdra, E.; Vojtko, M.; Lisnichuk, M.; Čižmárová, E. The Influence of Reagents on the Shape, Stability, and Toxicity of AgNPs and Their Use to Produce Polymer-AgNPs Composites. *Metals* **2023**, *13*, 1996. https://doi.org/10.3390/met13121996

Academic Editors: Guy Louarn and Eric Hug

Received: 23 October 2023
Revised: 19 November 2023
Accepted: 7 December 2023
Published: 9 December 2023

Copyright: © 2023 by the authors. Licensee MDPI, Basel, Switzerland. This article is an open access article distributed under the terms and conditions of the Creative Commons Attribution (CC BY) license (https://creativecommons.org/licenses/by/4.0/).

1. Introduction

Silver nanoparticles are used in various fields such as electronics, healthcare, and consumer products. The electronics industry consumes silver nanoparticles on a large scale; its consumption can reach hundreds or thousands of kilograms per year. The healthcare industry is the second significant consumer of silver nanoparticles, where AgNPs are used in medical devices, wound dressings, disinfectants, and other applications. Overall, regardless of the area of application, nanoparticle production is constantly increasing.

There are several methods of nanoparticle synthesis. By the synthesis method, it is possible to influence the parameters of the synthesized nanoparticles such as the size, surface properties, shape, and even chemical composition of nanoparticles. Subsequently, nanoparticle parameters influence the possibilities of their application. Synthesis techniques can be generally divided into three methods: physical methods, chemical methods, and bio-assisted methods (green methods) [1,2].

One of the most exciting materials for production on the nanoscale is silver. Silver nanoparticles exhibit unique chemical, optical, physical, and toxic properties. The first thing that draws attention to colloids of precious metals is their brilliant colors. Such unique optical properties are due to their plasmonic behavior resulting from the collective oscillation of their conduction band electrons [3]. The resonant frequency of this oscillation is highly dependent on the size and shape of the nanoparticle [4]. The resonance frequency of spherical nanoparticles is relatively constant; therefore, colloids of silver nanoparticles with a spherical shape, are usually yellow or red, while nanoparticles with a rod shape can appear green, blue, or purple. The resonance frequency of rod-shaped nanoparticles is highly dependent on the aspect ratio (i.e., length-to-width ratio) of the particle. Triangular or hexagonal silver nanoparticles can also produce a range of colors, from blue to orange [5].

By controlling the shape, size, and aspect ratio of the nanoparticles, the absorption and scattering of light can be tuned, which is important in specifying the optical properties. Also, other properties can be influenced by nanoparticles' shape. For instance, silver nanowires are excellent conductors of both electrons and photons, opening intriguing possibilities for electro-optical devices that have yet to be explored [6]. Triangular silver nanoparticles have a high surface-enhanced Raman scattering enhancement factor due to their sharp corners and edges, which can amplify the Raman scattering signal of molecules adsorbed on their surface. This makes them useful in chemical sensing, bioimaging, and forensic analysis applications. Triangular silver nanoparticles can also be used in plasmonic photothermal therapy, which involves heating cancer cells using near-infrared light. They can be successfully used in drug delivery and environmental monitoring applications.

The shape of AgNPs also impacts their interaction with biological systems. For example, rod-shaped AgNPs have been shown to have improved cellular uptake and enhanced therapeutic efficacy compared to spherical AgNPs due to their ability to penetrate cell membranes [7]. AgNPs can also be used as efficient catalysts (reduction of nitro compounds, oxidation of alcohols, and hydrogenation of olefins) due to their high surface area, shape-dependent electronic properties, and ability to adsorb molecules on their surface [8,9]. Triangular AgNPs, for instance, have been shown to exhibit higher catalytic activity than spherical AgNPs due to their high density of {111} facets [10]. The need for different shapes of AgNPs arises from the desire to tailor their properties to specific applications. By controlling the size and shape of AgNPs, achieving enhanced performance in a wide range of fields is possible.

The aim of this work was to synthesize silver nanoparticles of different shapes. We analyzed the influence of the reducing agent on the nanoparticles' shape change and the influence of the combination of trisodium citrate (TSC) and polyvinylpyrrolidone (PVP) on the capability to provide a non-toxic layer on the surface of the nanoparticles to minimize the toxic properties of AgNPs and the stabilizing/capping capability, to secure the stability of the nanoparticles. The non-toxic properties of prepared nanoparticles were evaluated against bacteria and green algae. The next goal was to prepare polymer–silver nanoparticle composite thin layers and fibers (nonwoven textiles).

2. Materials and Methods

2.1. Materials

Silver nitrate ($AgNO_3$, >98%) purchased from Mikrochem Ltd., Pezinok, Slovakia, was used as a silver precursor. Sodium borohydride ($NaBH_4$, ≥98%), TSC ($Na_3C_6H_5O_7$, ≥99%), hydrogen peroxide (H_2O_2, 30%), and PVP ($(C_6H_9NO)_n$, M.W. approx. 360,000) were also purchased from Mikrochem Ltd., Pezinok, Slovakia, and used as received. De-ionized water was used for preparing all solutions.

2.2. Chemical Synthesis of Silver Nanoparticles

Silver nanoparticles were synthesized using a chemical method, by reduction of Ag^+ ions to Ag^0. The concentrations and volumes of the used solutions are presented in Table 1.

Table 1. Concentrations of the reagents.

Reagents	Chemical Formula	Concentration	Volume (mL)
silver nitrate	$AgNO_3$	0.11 mM	100
sodium citrate	$Na_3C_6H_5O_7$	30 mM	8.56
polyvinylpyrrolidone	$(C_6H_9NO)_n$	2% *w*/*w*	8.56
hydrogen peroxide	H_2O_2	30%	0.28
sodium borohydride	$NaBH_4$	0.1 M	0.35; 0.37; 0.4; 0.47; 0.58; 0.7

All reagents were freshly prepared and added to $AgNO_3$ solution under constant stirring, in 1 min intervals, in the following order (except sample Ag4): TSC, PVP, H_2O_2, and $NaBH_4$. After all the reagents were added, the solutions were covered and stirred for 25 min in the dark. The difference between the solutions was in the volume of sodium borohydride; the labeling of the solutions is shown in Table 2. Sample Ag4 was prepared similarly but without TSC, and H_2O_2 was added. The prepared colloids were stored at room temperature in daylight.

Table 2. Labeling of solutions.

Sample	Volume of $NaBH_4$ (mL)	Note
Ag1	0.35	all reagents
Ag2	0.37	all reagents
Ag3	0.4	all reagents
Ag4	0.47	except for TSC and H_2O_2
Ag5	0.58	all reagents
Ag6	0.7	all reagents

2.3. PVA-AgNP Preparation

PVA-AgNP composites were prepared using the ex situ method. To concentrate the nanoparticles, the selected colloidal AgNP solutions were centrifuged. Specifically, 1000 mL of a colloidal solution of silver nanoparticles was centrifuged in several cycles. One cycle consisted of centrifuging six tubes (each of 50 mL) of the colloid; after the cycle was finished, most of the liquid was removed, and only a small part remained, which contained concentrated nanoparticles; specifically, we took approximately 40 mL from the 50 mL, and 10 mL with concentrated particles remained in the tube. Another part of the colloid was added to this volume in the next cycle, and the centrifugation was repeated. We topped up the sample until the entire content was concentrated (we obtained 150 mL of concentrate from 1000 mL of AgNP solution). The prepared concentrated solutions of nanoparticles were added to the PVA solution in such a proportion that an 8% aqueous solution of PVA-AgNPs was formed.

PVA-AgNP composite solutions were used to prepare the composite thin layers by casting at ambient temperature and nonwoven textiles prepared by a needleless electrospinning technique (Nanospider, NS LAB 200, Elmarco, Czech Republic). In the electrospinning, the applied voltage was 82 kV, and the distance between the spinning and collector electrodes was 150 mm.

2.4. Methods

The synthesized AgNPs were monitored using a UV-VIS spectrophotometer (GENESYS™ 180 UV-Vis Spectrophotometer, Thermo Fisher Scientific Inc. Madison, WI, USA). The size and morphology of the nanoparticles were studied using TEM (JEOL model JEM-2000FX, JEOL Company (USA) Inc., Peabody, MA, USA, an accelerating voltage of 200 kV) and SEM/FIB (SEM/FIB ZEISS-AURIGA Compact, Jena, Germany). The samples for TEM analysis were prepared by dropping the prepared colloidal solution onto a Cu grid covered with a carbon membrane. Energy-dispersive X-ray spectroscopy and electron diffraction were used to prove the presence of silver in nanoparticles. The samples for SEM analysis were

prepared by vaporization of carbon. Image analysis (ImageJ software, the National Institutes of Health and the Laboratory for Optical and Computational Instrumentation (LOCI, University of Wisconsin, Madison, WI, USA)) was used to analyze the Ag nanoparticles' size distribution.

2.5. Toxicity

The toxicity (antimicrobial and antibiofilm activity) of colloidal AgNPs was evaluated using the standard disk diffusion method with some modifications. One-cell green algae *Chlorella kessleri* (*Ch. kessleri*) was used for testing.

The agar disc diffusion test is the official method used in many clinical microbiology laboratories for routine testing [11]. In this procedure, agar plates were inoculated with the test microorganism (*Ch. kessleri*). Then, sterile swabs (~6 mm in diameter) containing the test compound (~15 µL) were placed on the agar surface. The Petri dishes were incubated at room temperature under light conditions of 12 h light and 12 h dark for 14 days. The antimicrobial agent diffused into the agar and inhibited the germination and growth of the test microorganism, and then the diameters of growth inhibition zones were measured.

3. Results and Discussion

After the components were added and mixed for 25 min, all of the solutions were removed from the stirrer and stored in daylight at ambient temperature. The first evidence of the successful synthesis of AgNPs was the coloring of the solutions (Figure 1a); a different color indicates the formation of nanoparticles of different shapes. To prove the presence of AgNPs in the solution and analyze the colloids, UV-VIS spectrophotometry was used (Figure 1b).

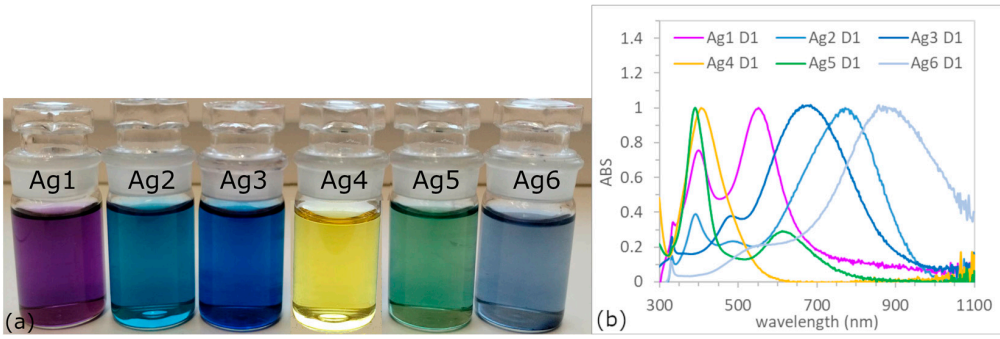

Figure 1. The color (**a**) and UV-VIS spectra (**b**) of colloidal solutions on the first day (D1) after synthesis.

UV-VIS spectrophotometry is a widely used method for analyzing colloidal solutions. Based on the shape of the spectrum, peak position, and number of peaks, it is possible to predict the size and shape of synthesized nanoparticles. The prepared solutions show spectra in the range of 330–822 nm (Figure 1b). All of the solutions can be divided into three groups based on the number of peaks:

- One peak—solution Ag4 (yellow solution);
- Three peaks—solutions Ag1, Ag3, Ag5, and Ag6 (purple, dark blue, green, and baby blue solutions);
- Four peaks—solution Ag2 (light blue solution).

The yellow colloid Ag4 shows just one strong peak at 406 nm (Figure 1b). It is well known that a spectrum with one sharp peak in the range of 380–420 nm indicates spherical silver nanoparticles [12,13]. Based on the one peak, with good symmetry and slimness, it can be concluded that our nanoparticles will be in a very narrow size interval. TEM analysis confirmed the presence of spherical nanoparticles with an average diameter of 12 nm (Figure 2d).

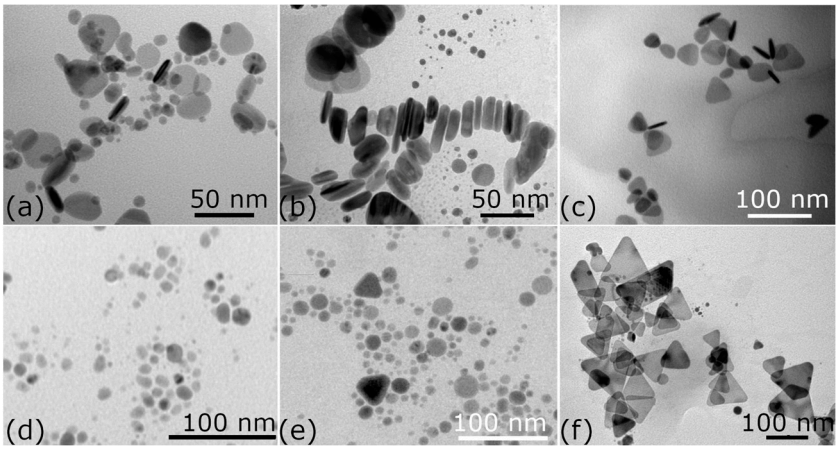

Figure 2. TEM micrographs of AgNP samples: Ag1 (**a**); Ag2 (**b**); Ag3 (**c**); Ag4 (**d**); Ag5 (**e**); Ag6 (**f**).

To confirm the presence of silver (sample Ag4), several techniques such as energy-dispersive X-ray spectroscopy, diffraction analysis, and a digital method for lattice fringe spacing measurements in HRTEM were used. Figure 3 shows the results of energy-dispersive X-ray spectroscopy of sample Ag4; it is evident that a strong silver signal is presented in Figure 3 (Spectra 1 and 2). The AgNP-free region (Spectrum 4) was measured to explain the presence of elements such as Si and Cu that appeared in the results. It is obvious that they do not belong to nanoparticles, but they are artifacts from the copper grid and possibly impurities on the C membrane.

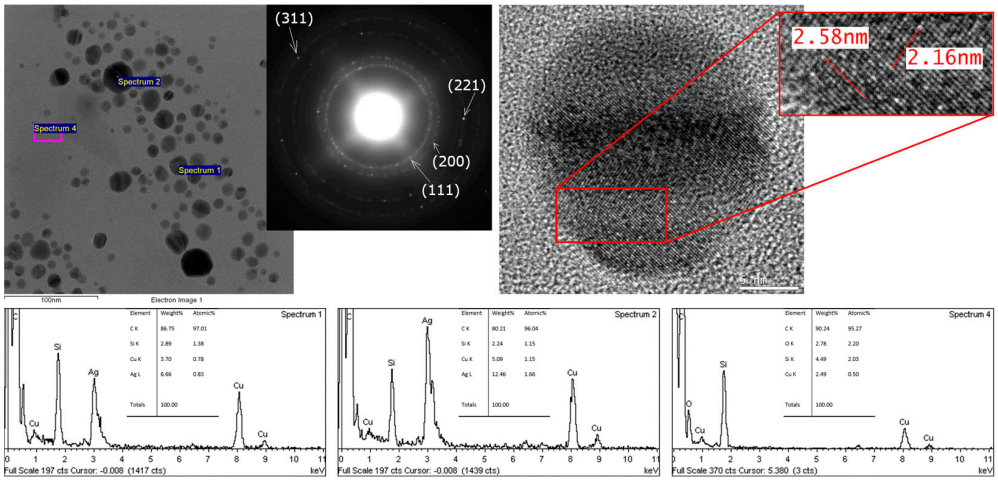

Figure 3. The energy-dispersive X-ray spectroscopy, electron diffraction of AgNPs, and structural lattice and lattice fringes of the synthesized AgNPs of sample Ag4.

Figure 3 also shows the electron diffraction pattern of the selected area of sample Ag4 and a high-resolution transmission electron micrograph of an isolated nanoparticle. The characteristic reflections of face-centered cubic crystalline silver are shown. Circular rings assigned to (111), (200), (220), and (311) can be observed. The HR-TEM image in Figure 3 shows the lattice fringe, which also confirms the crystalline nature of the synthesized AgNPs. The same analyses were performed for all samples, and in all, silver nanoparticles were confirmed. Here we show the results of selected samples, namely Ag4 (Figure 3), Ag5 (Figure 4), and Ag6 (Figure 5), as representative.

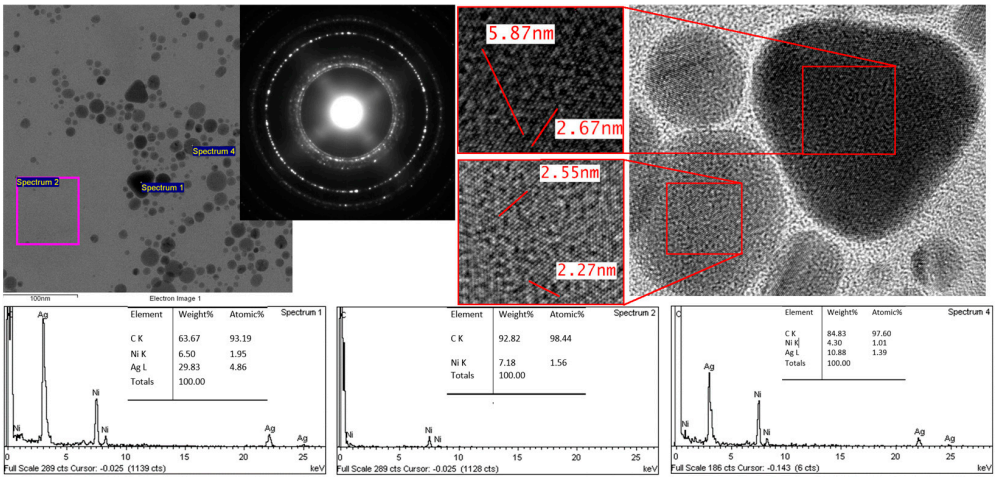

Figure 4. The energy-dispersive X-ray spectroscopy, electron diffraction of AgNPs, and structural lattice and lattice fringes of the synthesized AgNPs of sample Ag5.

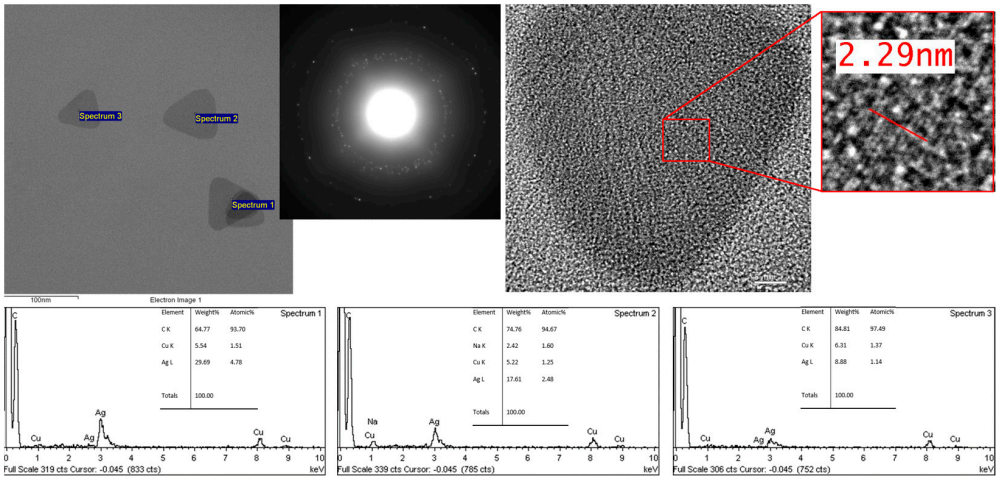

Figure 5. The energy-dispersive X-ray spectroscopy, electron diffraction of AgNPs, and structural lattice and lattice fringes of the synthesized AgNPs of sample Ag6.

The purple solution Ag1 shows a small sharp peak at 334 nm and two strong distinctive peaks at 400 and 552 nm (Figure 1b). TEM analysis showed the presence of three different shapes of the AgNPs: small spherical, with a mean diameter of 8 nm; truncated triangular or octahedral nanoparticles with a mean size of 25 nm; and rodlike nanoparticles with a length of ~24 nm (aspect ratio of 3:1) (Figure 2a). Spherical nanoparticles were the most represented, followed by truncated triangular nanoparticles, and only about 5% were rod-shaped nanoparticles.

The UV-VIS spectra of colloids Ag2 and Ag3 (light and dark blue solutions) show very similar spectra (Figure 1b); the spectrum of the Ag3 colloid missed the peak connected to spherical nanoparticles at ~400 nm. TEM analysis of Ag2 shows the presence of small spherical nanoparticles with a mean diameter of 10 nm, irregularly shaped triangles with a mean size of 40 nm, and rods with a length of ~33 nm (aspect ratio of 3:5:1) (Figure 2b). Particle analysis of the Ag3 sample shows triangles or rather rounded triangles of 30 nm in size, and 30 nm rods with an aspect ratio length to diameter of 4:1; no spherical nanoparticles were observed (Figure 2c).

The green solution Ag5 shows two peaks: at 390 and 612 nm (Figure 1b). TEM analysis (Figure 2e) shows the presence of spherical nanoparticles with a mean diameter of 10 nm and a small portion of triangular nanoparticles with a mean size of 44 nm. Figure 5 shows energy-dispersive X-ray spectroscopy, diffraction analysis, and a digital method for lattice

fringe spacing measurements in HRTEM that confirm that the prepared nanoparticles are silver.

The Ag6 solution (baby blue) showed a peak at 330, a small one more like a shoulder at 556, and a distinctive peak at 882 nm (Figure 1b). Based on [14,15], it can be concluded that with the presence of a peak with ABS_{max} at a wavelength of more than 800 nm, triangular nanoparticles can be expected. TEM analysis confirmed the presence of triangular prisms with a mean size of 59 nm (size interval from 30 to 112 nm). Figure 5 shows the analyses which confirmed the silver in the prepared nanoparticles.

Based on UV-VIS spectra and TEM analysis of AgNPs, it can be concluded that all colloids where spectra show ABS_{max} around 400 nm contain spherical nanoparticles. Spectra with ABS_{max} above 500 nm indicate the presence of triangles, and the higher the wavelength of the peak (Figure S1), the greater the representation of triangular prisms in the colloid.

If there is a significant peak at ~500 nm, rods may be present in the solution, but this peak must also be perceived in combination with a peak at higher wavelengths; if such occurs, triangular prisms will be present in the solution, not rods. The more the maxima are shifted to higher wavelengths, the sharper the triangles [16].

The results showed that predicting the growth mechanism of nanoparticles and/or shape formation mechanisms is not an easy task. It is obvious that the ratio between the reactants is a key factor and fundamentally affects the mechanism of nanoparticle formation even when there are tiny changes in the volume of the reducing agent. We found that with the increase in the volume of $NaBH_4$ in the colloid, the representation of triangular nanoparticles increases (with a volume of 0.7 mL of $NaBH_4$, there are only triangular prisms in the colloid). However, this is only true if all reactants participate in the reaction. For example, if TSC and H_2O_2 are missing, only spherical nanoparticles are formed. In the literature, it is possible to find several possible growth mechanisms of plate (triangular prisms) or spherical AgNPs. However, these experiments showed that the shape formation mechanisms change with changing experimental conditions, which means that all proposed mechanisms are valid for a particular synthesis process.

3.1. Influence of Reagents on AgNP Synthesis

The silver nanoparticle synthesis process is very sensitive to many conditions (light, stirring, temperature, etc.) but mainly to the type and volume of added reagents. The most used reagents for the chemical synthesis of AgNPs are $NaBH_4$, TSC, PVP, and H_2O_2. Each reagent added to the silver nitrate solution plays an important role and influences the size and shape of synthesized nanoparticles. The prepared colloidal solutions (sample Ag1–Ag6) differ in the volume of $NaBH_4$ added (Table 1), and as can be seen in Figure 1a, even the difference of a few tenths of microliters caused substantial changes in the color of the solutions.

$NaBH_4$, as a strong reducing agent, influenced the synthesis and the shape of AgNPs. The chemical reaction of Ag^+ ions into elementary silver Ag^0 in the presence of $NaBH_4$ can be described by the following reaction [17]:

$$2AgNO_{3(aq)} + 2NaBH_{4(aq)} \rightarrow 2Ag^0 + B_2H_{6(g)} + 2NaNO_{3(aq)} + H_{2(g)} \uparrow \quad (1)$$

The reduction rate of $NaBH_4$ is very fast; the change in color can be observed immediately after the addition of $NaBH_4$ into the solution. It is well known that strong reducing agents have high nucleation ability and favor the formation of many small nanoparticles. Stabilizing agents must be added to prevent particle agglomeration or growth. In addition, sodium borohydride has one significant disadvantage: the solution of $NaBH_4$ must be prepared fresh daily. An analysis of the influence of the borohydride solution age on the formation of silver nanoprisms was performed by Frank et al. [13]. Sodium borohydride decomposes in water as follows:

$$NaBH_{4(aq)} + 4H_2O_{(l)} \leftrightarrow Na[B(OH)_4]_{(aq)} + 4H_{2(g)} \quad (2)$$

Frank et al. found that the borohydride water solution can be successfully used within 20 h.

TSC and PVP are considered weak reducing agents [18–20]; their capability to reduce Ag^+ ions to Ag^0 can be expressed by chemical Equations (3) and (4):

$$4Ag^+ + Na_3C_6H_5O_7 + 2H_2O \rightarrow 4Ag^0 + C_6H_5O_7H_3 + 3Na^+ + H^+ + O_2\uparrow \quad (3)$$

$$2Ag^+ + (C_6H_9NO)_n \rightarrow 2Ag^0 + C_6H_6O_6 + 2H^+ \quad (4)$$

TSC is mostly a stabilization agent; Gontijo et al. report that TSC provides surface ligands [21]. TSC gives a negative charge to AgNPs (electrostatic repulsion). Since the silver colloidal particles possessed a negative charge, a repulsive force worked against the particles and prevented aggregation. It can also be concluded that TSC is a very important reactant in the process of nanoparticle shape influence. The latest research on citrate impact shows that citrate ions alone can stabilize silver nanoplates by stabilizing silver nuclei through preferential binding to the {111} planes [22]. However, its stabilization effect must be supported by another ligand. The combination of citrate and PVP helps to stabilize and control the formation of nanoparticles' shape. Tao et al. found that the ratio between Ag^+ and the number of repeating units of PVP defined the geometry of NPs [23]. PVP provides covalent organic ligands and allows steric repulsion to prevent AgNP aggregation; moreover, it can protect AgNP surfaces from oxidation and instability [24]. Thiele et al. [25] analyzed the influence of PVP content on nanoparticle synthesis and proved that even a low concentration of PVP could ensure well-dispersed silver nanoparticles. There is no doubt that PVP is a successful shape control agent for fcc metals. Li et al. tested the effect of varying amounts of PVP on nanoparticle shape formation and found that triangular prisms were more likely to form as the volume of PVP increased [26]. They also proposed a possible mechanism for the growth of plate-shaped silver particles and confirmed that most of the PVP is absorbed in the (111) plane, which promotes the absorption of Ag atoms in the (110) planes and the formation of plate-shaped nanoparticles.

The impact of H_2O_2 on silver ions strongly depends on the pH of the solution [27–29]. H_2O_2 can act as a reducing agent under alkaline conditions [28]. When Ag nanoparticles and H_2O_2 are mixed under neutral conditions, H_2O_2 acts as an oxidizing agent and the surface of Ag nanoparticles can be dissolved. H_2O_2 is known to etch silver nanoparticles with selective preservation of the Ag{111} plane [28]. It was proved that H_2O_2 can change the shape of already synthesized nanoparticles by etching [22,30,31]. The reaction between H_2O_2 and Ag^0 can be expressed by reaction (5):

$$2Ag^0{}_{(s)} + H_2O_{2(aq)} + 2H^{2+}{}_{(aq)} \leftrightarrow 2Ag^+{}_{(aq)} + 2H_2O_{(l)} \quad (5)$$

Frank et al. conclude that less stable newly formed silver nanoparticles are etched by hydrogen peroxide, establishing an equilibrium between sodium borohydride reduction and hydrogen peroxide oxidation of silver [13]. Based on these findings, it can be expected that different volumes of $NaBH_4$ with the same amount of H_2O_2 may influence the resulting shape of the nanoparticles.

One reason for interest in creating different shapes of silver nanoparticles arises from their catalytic ability. It is proven that nanoparticles of different shapes have different reactivities due to the presence of different crystalline facets. For example, Xu et al. demonstrated that Ag nanocubes with predominantly {100} planes were significantly more active in oxidation than nanoplates with predominantly {111} planes, while nanospheres containing a combination of both crystal facets showed intermediate reaction rates [16].

The influence of individual reactants must be considered in the context of other reactants used in the synthesis. The combination of several agents brings a change to the system, and it is not possible to clearly divide the functions of individual reactants. Therefore, we studied the influence of the volume of the strongest reducing agent on the shape change of nanoparticles.

3.2. Toxicity of Silver Nanoparticles

The main mechanisms of AgNP toxicity in living cells have been proposed and analyzed by many authors [16,32–34]. Nanoparticles can have a toxic effect on cells through three mechanisms: oxidative stress, DNA damage, and reproductive disorders. It is well known that AgNPs are toxic mainly if they are not properly stabilized or if they are used at high concentrations.

The degree of antibiofilm/toxic effect of prepared nanoparticles on green algae *Ch. kessleri* expressed by the size of inhibition zones is shown in Table 3.

Table 3. Antibiofilm effect of prepared nanoparticles determined by the diameter of the inhibition zone tested on green algae *Ch. kessleri*.

	Ag1	**Ag2**	**Ag3**	**Ag4**	**Ag5**	**Ag6**	**$AgNO_3$ Solution**
IZ (mm)	7.5	7	7.5	7	7	8	12

After 14 days of cultivation, the maximum inhibition zone caused by AgNPs was measured on sample Ag6 (8 mm in diameter). The $AgNO_3$ solution (Table 3) showed a clear inhibition zone of 12 mm, which proved that Ag^+ ions have a very good toxic effect. All inhibition zones are shown in Figure S2.

With proper stabilization of the nanoparticles [35], there is a low probability of Ag^+ ion release from AgNPs. Surface modification by coating the AgNPs with biocompatible or biodegradable materials, such as polymers (PVP, polyethylene glycol (PEG), and chitosan) [36] or proteins, can prevent direct contact between the nanoparticles and living cells, reducing potential toxicity. The toxicity can also be controlled by the size and shape of nanoparticles. Surface charge manipulation is the next possibility for influencing the toxicity. Modifying the surface charge of AgNPs can influence their interactions with cells and tissues (enhance biocompatibility and reduce toxicity). The choice of surface coating for AgNPs depends on the specific application and the desired properties of the nanoparticles.

The reason why our AgNPs are not highly toxic is that they have low solubility because of the good coating/stabilizing effect caused by the combination of the TSC and PVP. TSC provides the negative charge on AgNPs' surfaces which prevents their agglomeration due to the generation of repulsion force between AgNPs. Behera et al. proposed a mechanism of PVP and nanoparticle interaction. According to it, an electron-rich PVP molecule is adsorbed readily onto a metal surface via n-electrons of C=O groups and forms a "core–shell" structure with a nanoparticle core covered by an amorphous PVP surface layer [37].

Studies have shown that AgNPs also exhibit dose-dependent toxicity, increasing their toxicity with increasing concentrations [38]. The concentration and stabilization of the AgNP surface are key factors, but it was found that the shape of AgNPs is also one of the important factors. In the literature, many works dealing with shape versus toxicity issues can be found, and it was proved that some shapes are more toxic than others. Spherical AgNPs have been shown to have lower toxicity compared to other shapes. The reason is that spherical AgNPs have a low surface-area-to-volume ratio, which reduces their ability to interact with biological molecules and cells. Rod-shaped AgNPs are more toxic than spherical ones. This is thought to be because the rod shape allows them to penetrate cells more easily, leading to increased cellular damage. Triangular AgNPs are the most toxic shape of AgNPs. This is thought to be because the sharp edges and corners of the triangles can cause physical damage to cells and tissues. Also, the release of silver ions from triangular corners is more likely than that from the surface of spherical nanoparticles. The size of the nanoparticles is also very important; this fact is also confirmed by Penghui et al. in their work [39].

From our results, it is clear that, despite the primary toxicity, silver nanoparticles can potentially be used safely if properly stabilized. Non-toxic AgNPs can find applications in medicine and can be functionalized or loaded with various active ingredients such as drugs, antimicrobial agents, or growth factors. Non-toxic AgNPs allow controlled and

targeted release of these substances, ensuring effective delivery while minimizing potential toxicity to healthy cells.

3.3. PVA-AgNP Composites

We supposed that the incorporation of AgNPs into the polymer matrix allows their properties to be transferred to the polymer, and such a material can exhibit unique properties that the individual components do not have on their own. The PVA-AgNP composites were prepared using nanoparticles synthesized in samples Ag4 and Ag6, which contained nanoparticles of one shape: spherical and triangular. Both prepared composite solutions (Figure 6a) were used for electrospinning of fibers (nonwoven fabrics) (Figure 6b,d) and the production of thin composite layers by casting (Figure 6c,e). It is obvious that the addition of the Ag4 sample caused a distinctly yellow coloration, and Ag6 caused a blue coloration of the colorless PVA matrix.

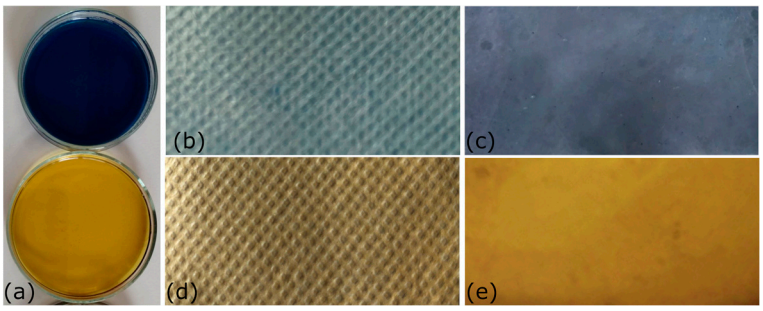

Figure 6. The Petri dishes with cast PVA-AgNP composite solutions of Ag6 (blue solution, triangular nanoparticles) and Ag4 (yellow solution, spherical nanoparticles) (**a**); nonwoven textiles and cast thin composite layers with incorporated Ag6 (**b**,**c**) and Ag4 (**d**,**e**) nanoparticles.

Figure 7 shows the details of the yellow polymer fibers at different magnifications. Figure 7a shows a microphotograph taken at 50× magnification, and Figure 7b,c show SEM microphotographs; it is obvious that electrospinning is a suitable technique for producing nonwoven textiles, and the diameter of fibers was in the interval from 0.3 µm to 2 µm.

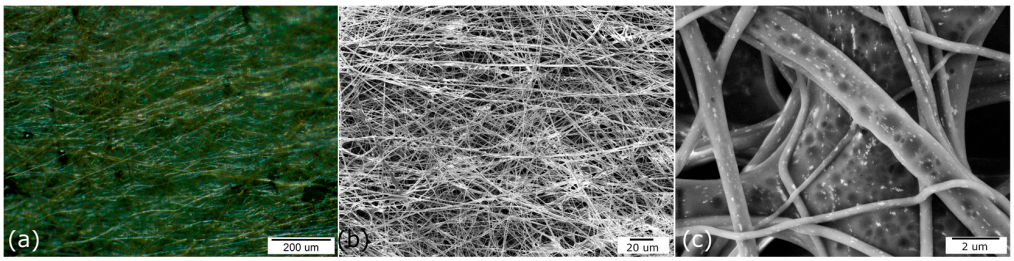

Figure 7. Microphotograph of PVA-AgNP fibers prepared by incorporation of nanoparticles of sample Ag4 (**a**), SEM microphotograph of the same sample (**b**), and detail of AgNPs' distribution in fibers (**c**).

The properties of polymer–silver composites mainly affect the distribution of nanoparticles. Figure 7c shows that the added silver nanoparticles mostly form clusters (chains of nanoparticles); clusters were also observed in thin layers, and we assume that it was the electrostatic spinning that caused the redistribution of clusters into chains. A more even distribution of nanoparticles could be achieved by more intense mixing, increasing the temperature during mixing, and using ultrasound.

Nanoparticles undoubtedly enrich the polymer with their properties; therefore, polymer–silver nanoparticle composites have a wide range of applications across various fields: sensors, electronic and optoelectronic devices, water purification (filter materials), catalysis, biomedicine, packaging materials, and so on.

3.4. Long-Term Stability of the Colloidal Solutions

The color of all of the solutions (Figure 8a) and the UV-VIS spectra (Figure 8b) after two months of storage in daylight show some significant changes in the colloidal solutions, except for the Ag4 and Ag5 solutions.

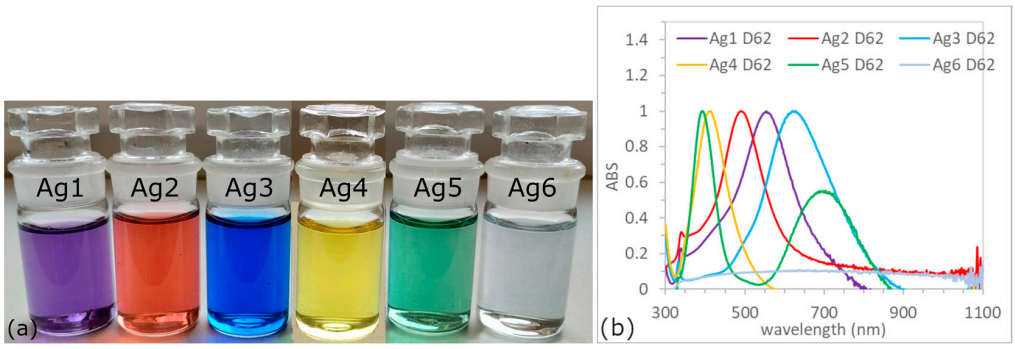

Figure 8. Color of the solutions (**a**) and UV-VIS spectra (**b**) after two months (62 days).

The absence of a change in the UV-VIS spectrum (Figure 9a) indicates stable nanoparticles, and the TEM analysis of the Ag4 colloid confirmed the presence of spherical nanoparticles with unchanged size. The second most stable solution was the Ag5 solution. The UV-VIS spectrum of the Ag5 solution (Figure 9b) showed just a little change in the position of the second peak. After two months, a mixture of triangular and spherical nanoparticles with an unchanged size was proved by TEM analysis. Also, a small amount of truncated triangular nanoparticles was observed. The shift of the second peak can be explained by the appearance of truncated triangles.

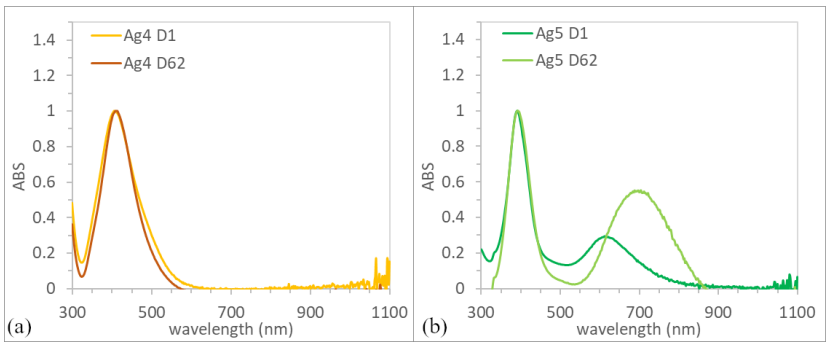

Figure 9. Comparison of the UV-VIS spectra of Ag4 (**a**) and Ag5 (**b**) solutions on D0 and D62.

In the case of the other samples (Ag1, 2, and 3), there is a clear change in solution colors on the first day (Figure 1b) compared to day 62 (Figure 8b). Such changes indicate a change in the shape of the nanoparticles. In all these samples, only rod-shaped and spherical nanoparticles were observed in the TEM micrographs of the samples after 62 days (Figure 10). The difference between individual samples was in the ratio of spheres to rods, and as the wavelength of ABS_{max} increased, a decrease in the ratio of spheres to rods was observed. We assume that the presence of H_2O_2 affected the shape of the nanoparticles. Such an effect of H_2O_2 was observed and analyzed by Raza et al. in their work [16].

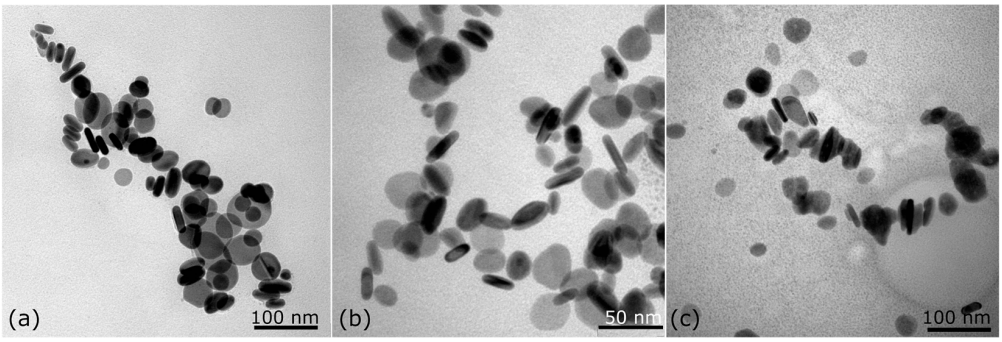

Figure 10. TEM microphotographs of nanoparticles in colloids Ag1 (**a**), Ag2 (**b**), and Ag3 (**c**) after two months.

Ag nanoparticles are known to be sensitive to light. Lee et al. observed the influence of light conditions on the shape of nanoparticles [32]. The authors proved the switchable photomorphic properties of AgNPs. Nanoprisms were found to reversibly transform into disc-shaped morphologies when placed in the dark, with subsequent exposure to light resulting in the return of triangular prism-shaped morphologies. These transitions between triangular prisms and discs were found to be switchable over multiple cycles. We assume that the oxidizing effect of H_2O_2 and daylight influences the process of shape changing in our colloids, but it is not reversible in our case.

The most significant change was observed in the case of the Ag6 colloid; after three months, no nanoparticles were observed, and the color of the solution changed to transparent/pure. The broad UV-VIS spectrum of the Ag6 colloid indicates the degradation of the nanoparticles. We assume that the dissolving of nanoparticles occurred because stabilizing agents were not able to secure long-term stability.

4. Conclusions

We have successfully prepared AgNPs with different shapes. Our results confirmed that $NaBH_4$ is a key factor in AgNPs' shape-changing process. In general, spherical nanoparticles cause a yellow color, and solely triangular nanoparticles cause a blue color of the solution. If there is a mixture of nanoparticles of different shapes in the colloid, the color depends on the size and mutual ratio of the individual shapes. Also, it was found that the nanoparticles stabilized by PVP and TSC have very low, almost negligible toxic effects against bacteria and algae. It was also proven that PVP and TSC, in contrast to antibacterial properties, are not able to ensure the long-term stability of AgNP colloidal solutions. We proved that daylight and H_2O_2 are key factors that affect the long-term stability of AgNPs. Further investigations are needed to better understand the influence of reactants on nanoparticle shape formation (under certain conditions) and also to understand the coating/encapsulation mechanisms and their effect on the toxicity and/or toxicity control of AgNPs.

We have successfully prepared polymer–silver nanoparticle composites and proved that adding AgNPs significantly influences polymer matric properties. The versatile nature of polymer–silver nanoparticle composites makes them valuable in many industries, and ongoing research continues to uncover new applications and potential uses for these materials.

Supplementary Materials: The following supporting information can be downloaded at https://www.mdpi.com/article/10.3390/met13121996/s1: Figure S1: Comparison of UV-vis spectra of samples Ag2, Ag3 and Ag6; Figure S2: The anti-biofilm effect of AgNPs colloidal solution: Ag1(a); Ag2(b); Ag3(c); Ag4(d); Ag5(e) Ag6(f), $AgNO_3$ solution (g) and control with water (h) on *Ch. kessleri* (sterile swabs diameter was 6 mm in all tests).

Author Contributions: Conceptualization, O.V. and L.M.; methodology, O.V., L.M., V.M., M.V., M.L. and E.M.; validation, O.V., E.M. and E.Č.; formal analysis, L.M., E.Č. and V.M.; investigation, O.V., M.V., V.M., L.M., M.L. and E.Č.; data curation, O.V. and L.M.; writing—original draft preparation, O.V.; visualization, E.Č. and L.M. All authors have read and agreed to the published version of the manuscript.

Funding: This research received no external funding.

Data Availability Statement: The data presented in this study are available from the corresponding author, upon reasonable request.

Acknowledgments: This work was supported by the Slovak Grant Agency (VEGA 1/0020/22).

Conflicts of Interest: The authors declare no conflict of interest.

References

1. Dhand, C.; Dwivedi, N.; Loh, X.J.; Jie Ying, A.N.; Verma, N.K.; Beuerman, R.W. Methods and strategies for the synthesis of diverse nanoparticles and their applications: A comprehensive overview. *RSC Adv.* **2015**, *5*, 105003–105037. [CrossRef]
2. Hutter, E.; Fendler, J.H. Exploitation of Localized Surface Plasmon Resonance. *Adv. Mater.* **2004**, *16*, 1685–1706. [CrossRef]
3. Xia, Y.; Halas, N.J. Shape-Controlled Synthesis and Surface Plasmonic Properties of Metallic Nanostructures. *MRS Bull.* **2005**, *30*, 338–348. [CrossRef]
4. Sun, Y.; An, C. Shaped gold and silver nanoparticles. *Front. Mater. Sci.* **2010**, *5*, 1–24. [CrossRef]
5. Kelly, K.L.; Coronado, E.; Zhao, L.L.; Schatz, G.C. The Optical Properties of Metal Nanoparticles: The Influence of Size, Shape, and Dielectric Environment. *J. Phys. Chem. B* **2003**, *107*, 668–677. [CrossRef]
6. Wiley, B.; Sun, Y.; Xia, Y. Synthesis of Silver Nanostructures with Controlled Shapes and Properties. *Acc. Chem. Res.* **2007**, *40*, 1067–1076. [CrossRef]
7. Huang, X.; Li, L.; Liu, T.; Hao, N.; Liu, H.; Chen, D.; Tang, F. The Shape Effect of Mesoporous Silica Nanoparticles on Biodistribution, Clearance, and Biocompatibility in Vivo. *ACS Nano* **2011**, *5*, 5390–5399. [CrossRef] [PubMed]
8. Silvestri, B.; Armanetti, P.; Sanità, G.; Vitiello, G.; Lamberti, A.; Calì, G.; Pezzella, A.; Luciani, G.; Menichetti, L.; Luin, S.; et al. Silver-nanoparticles as plasmon-resonant enhancers for eumelanin's photoacoustic signal in a self-structured hybrid nanoprobe. *Mat. Sci. Eng. C* **2019**, *102*, 788–797. [CrossRef]
9. Mostafa, S.; Behafarid, F.; Croy, J.R.; Ono, L.K.; Li, L.; Yang, J.C.; Frenkel, A.I.; Cuenya, B.R. Shape-Dependent Catalytic Properties of Pt Nanoparticles. *J. Am. Chem. Soc.* **2010**, *132*, 15714–15719. [CrossRef]
10. Xu, R.; Wang, D.; Zhang, J.; Li, Y. Shape-Dependent Catalytic Activity of Silver Nanoparticles for the Oxidation of Styrene. *Chem. Asian J.* **2006**, *1*, 888–893. [CrossRef]
11. Balouiri, M.; Sadiki, M.; Ibnsouda, S.K. Methods for in vitro evaluating antimicrobial activity: A review. *J. Pharm. Anal.* **2016**, *6*, 71–79. [CrossRef] [PubMed]
12. Deivaraj, T.C.; Lala, N.L.; Lee, J.Y. Solvent-induced shape evolution of PVP protected spherical silver nanoparticles into triangular nanoplates and nanorods. *J. Coll. Inter. Sci.* **2005**, *289*, 402–409. [CrossRef] [PubMed]
13. Frank, A.J.; Cathcart, N.; Maly, K.E.; Kitaev, V. Synthesis of Silver Nanoprisms with Variable Size and Investigation of Their Optical Properties: A First-Year Undergraduate Experiment Exploring Plasmonic Nanoparticles. *J. Chem. Educ.* **2010**, *87*, 1098–1101. [CrossRef]
14. Wang, H.; Cui, X.; Guan, W.; Zheng, X.; Zhao, H.; Wang, Z.; Wang, Q.; Xue, T.; Liu, C.; Singh, D.J.; et al. Kinetic effects in the photomediated synthesis of silver nanodecahedra and nanoprisms: Combined effect of wavelength and temperature. *Nanoscale* **2014**, *6*, 7295–7302. [CrossRef] [PubMed]
15. Xu, X.; Du, Z.; Wu, W.; Wang, Y.; Zhang, B.; Mao, X.; Jiang, L.; Yang, J.; Hou, S. Synthesis of triangular silver nanoprisms and spectroscopic analysis on the interaction with bovine serum albumin. *Anal. Bioanal. Chem.* **2017**, *409*, 5327–5336. [CrossRef] [PubMed]
16. Raza, M.; Kanwal, Z.; Rauf, A.; Sabri, A.; Riaz, S.; Naseem, S. Size- and Shape-Dependent Antibacterial Studies of Silver Nanoparticles Synthesized by Wet Chemical Routes. *Nanomaterials* **2016**, *6*, 74–82. [CrossRef]
17. Mirzaei, A.; Janghorban, K.; Hashemi, B.; Bonyani, M.; Leonardi, S.G.; Neri, G. Characterization and optical studies of PVP-capped silver nanoparticles. *J. Nanostr. Chem.* **2016**, *7*, 37–46. [CrossRef]
18. Ho, V.T.T.; Thi, N.D. Synthesis of Silver Nanoparticles via Chemical Reduction and its Anti-bacterial Activities in Wastewater of Shrimp Pond. *Int. J. Eng. Res. Technol.* **2016**, *5*, 1–5.
19. Rashid, M.U.; Bhuiyan, M.K.H.; Quayum, M.E. Synthesis of Silver Nano Particles (Ag-NPs) and their uses for Quantitative Analysis of Vitamin C Tablets. *Dhaka Univ. J. Pharmac. Sci.* **2013**, *12*, 29–33. [CrossRef]
20. Piñero, S.; Camero, S.; Blanco, S. Silver nanoparticles: Influence of the temperature synthesis on the particles' morphology. *J. Phys. Conf. Ser.* **2017**, *786*, 012020. [CrossRef]
21. Gontijo, L.A.P.; Raphael, E.; Ferrari, D.P.S.; Ferrari, J.L.; Lyon, J.P.; Schiavon, M.A. pH effect on the synthesis of different size silver nanoparticles evaluated by DLS and their size-dependent antimicrobial activity. *Rev. Matéria* **2020**, *25*, e12845. [CrossRef]

22. Zhang, Q.; Li, N.; Goebl, J.; Lu, Z.; Yin, Y. Systematic Study of the Synthesis of Silver Nanoplates: Is Citrate a "Magic" Reagent? *J. Am. Chem. Soc.* **2011**, *133*, 18931–18939. [CrossRef] [PubMed]
23. Tao, A.; Sinsermsuksakul, P.; Yang, P. Polyhedral silver nanocrystals with distinct scattering signatures. *Angew. Chem. Int. Ed.* **2006**, *45*, 4597–4601. [CrossRef] [PubMed]
24. Miesen, T.J.; Engstrom, A.M.; Frost, D.C.; Ajjarapu, R.; Ajjarapu, R.; Lira, C.N.; Mackiewicz, M.R. A hybrid lipid membrane coating "shape-locks" silver nanoparticles to prevent surface oxidation and silver ion dissolution. *RSC Adv.* **2020**, *10*, 15677–15693. [CrossRef] [PubMed]
25. Thiele, H.; von Levern, H. Synthetic protective colloids. *J. Colloid Sci.* **1965**, *20*, 679–694. [CrossRef]
26. Li, J.; Li, N.; Wan, x.; Xu, L.; Baral, A.; Chen, G.; Ju, S. Synthesis of monodispersed plate-shaped silver particles: With high tap-density and low radius-thickness ratio. *J. Mat. Res. Technol.* **2022**, *19*, 2497–2509. [CrossRef]
27. Nishimoto, M.; Abe, S.; Yonezawa, T. Preparation of Ag nanoparticles using hydrogen peroxide as a reducing agent. *New J. Chem.* **2018**, *42*, 14493–14501. [CrossRef]
28. Gatemala, H.; Pienpinijtham, P.; Thammacharoen, C.; Ekgasit, S. Rapid fabrication of silver microplates under an oxidative etching environment consisting of O_2/Cl^-, $NH_4OH/$ H_2O_2, and H_2O_2. *Cryst. Eng. Comm.* **2015**, *17*, 5530–5537. [CrossRef]
29. Gatemala, H.; Ekgasit, S.; Wongravee, K. High purity silver microcrystals recovered from silver wastes by eco-friendly process using hydrogen peroxide. *Chemosphere* **2017**, *178*, 249–258. [CrossRef]
30. Zannotti, M.; Vicomandi, V.; Rossi, A.; Minicucci, M.; Ferraro, S.; Petetta, L.; Giovannetti, R. Tuning of hydrogen peroxide etching during the synthesis of silver nanoparticles. An application of triangular nanoplates as plasmon sensors for Hg^{2+} in aqueous solution. *J. Molec. Liquids* **2020**, *309*, 113238. [CrossRef]
31. Oh, J.-H.; Kim, B.C.; Lee, J.-S. Colorimetric detection of acetylcholine with plasmonic nanomaterials signaling. *Anal. Bioanal. Chem.* **2014**, *406*, 7591–7600. [CrossRef] [PubMed]
32. Lee, G.P.; Minett, A.I.; Innis, P.C.; Wallace, G.G. A new twist: Controlled shape-shifting of silver nanoparticles from prisms to discs. *J. Mat. Chem.* **2009**, *19*, 8294. [CrossRef]
33. Navarro, E.; Piccapietra, F.; Wagner, B.; Marconi, F.; Kaegi, R.; Odzak, N.; Sigg, L.; Behra, R. Toxicity of silver nanoparticles to Chlamydomonas reinhardtii. *Environ. Sci. Technol.* **2008**, *42*, 8959–8964. [CrossRef] [PubMed]
34. Stensberg, M.C.; Wei, Q.; McLamore, E.S.; Porterfield, D.M.; Wei, A.; Sepúlveda, M.S. Toxicological studies on silver nanoparticles: Challenges and opportunities in assessment, monitoring and imaging. *Nanomedicine* **2011**, *6*, 879–898. [CrossRef] [PubMed]
35. Majeed, S.; Aripin, F.H.B.; Shoeb, N.S.B.; Danish, M.; Ibrahim, M.N.M.; Hashim, R. Bioengineered silver nanoparticles capped with bovine serum albumin and its anticancer and apoptotic activity against breast, bone and intestinal colon cancer cell lines. *Mat. Sci. Eng. C* **2019**, *102*, 254–263. [CrossRef] [PubMed]
36. Espinosa-Cristóbal, L.F.; Martínez-Castañón, G.A.; Loyola-Rodríguez, J.P.; Niño-Martínez, N.; Ruiz, F.; Zavala-Alonso, N.V.; Lara, R.H.; Reyes-López, S.Y. Bovine Serum Albumin and Chitosan Coated Silver Nanoparticles and Its Antimicrobial Activity against Oral and Nonoral Bacteria. *J. Nanomat.* **2015**, 420853. [CrossRef]
37. Behera, M.; Ram, S. Intense quenching of fluorescence intensity of poly(vinyl pyrrolidone) molecules in presence of gold nanoparticles. *Appl. Nanosci.* **2012**, *3*, 543–548. [CrossRef]
38. Ferdous, Z.; Nemmar, A. Health Impact of Silver Nanoparticles: A Review of the Biodistribution and Toxicity Following Various Routes of Exposure. *Int. J. Molec. Sci.* **2020**, *21*, 2375. [CrossRef]
39. Nie, P.; Zhao, Y.; Xu, H. Synthesis, applications, toxicity and toxicity mechanisms of silver nanoparticles: A review. *Ecotoxicol. Environ. Saf.* **2023**, *253*, 114636. [CrossRef]

Disclaimer/Publisher's Note: The statements, opinions and data contained in all publications are solely those of the individual author(s) and contributor(s) and not of MDPI and/or the editor(s). MDPI and/or the editor(s) disclaim responsibility for any injury to people or property resulting from any ideas, methods, instructions or products referred to in the content.